The 2009 IEEE/RSJ International Conference on
Intelligent Robots and Systems
October 11-15, 2009 St. Louis, USA

# Understanding the Common Principle underlying Passive Dynamic Walking and Running

Dai Owaki, Koichi Osuka, and Akio Ishiguro

*Abstract*— **In this study, we discuss the common stabilization mechanism underlying passive dynamic walking (PDW) and passive dynamic running (PDR), focusing on the feedback structures in analytical Poincaré maps. To this end, we have derived linearized analytical Poincaré maps for PDW and PDR, and analyzed these stabilities on two models, namely models with elastic elements and with stiff legs. Through our theoretical analysis, we have found an "implicit two-delay feedback structure", which can be seen as a certain type of two-delay input digital feedback control developed as an artificial control structure in the field of control theory, is an inherent stabilization mechanism in PDR appearing from the model with elastic elements, and two-period and four-period PDW appearing from with stiff legs. This mechanism is the key to adaptive function underlying phase transition phenomenon between PDW and PDR and period-doubling bifurcation phenomenon in PDW. To the best of our knowledge, this has not yet to be addressed and studied so far. Our results shed new light on the common underlying principle of passive dynamic locomotion, including biped PDW and PDR**

## I. INTRODUCTION

Passive dynamic walking (PDW) that has its roots in the pioneering research of McGeer [1], not only intrinsically offers nonlinear phenomena such as *pull-in effect* and *period-doubling bifurcation phenomenon* [2], [3], but also an extremely interesting phenomenon, leading to the engineering feasibility of highly efficient walking robot [4]. In recent years, several theoretical studies that attempt to elucidate the underlying principles of PDW have been reported [5], [6]. Using analytical Poincaré map, Sugimoto et al. [6] showed that *implicit feedback structure* present in Poincaré map contributes to the self-stability of PDW. Furthermore, feedback structures corresponding to one-period PDW, two-period PDW, and four-period PDW are implicit, and the bifurcation phenomenon is exhibited because of the actualization of the most stable structure in response to changes in ground slope angle [7]. Recently, by further developing the concept proposed by Sugimoto et al., Hirata [8] clearly showed that the stabilization mechanism in PDW corresponds to *cheap optimal control*.

However, all the above theoretical studies are related to biped PDW. The passive dynamic locomotion includes biped passive dynamic running (PDR) [9], [10]. The biped PDW is nothing more than a single form of locomotion. It is essential to discuss various types of locomotion including biped PDR as well as biped PDW, leading to the understanding the common underlying principle of passive dynamic locomotion, which in turn extracts design principles that form the core of adaptive legged locomotion. Moreover, using theoretical rationalization related to gait transition between PDW and PDR, it is expected that unprecedented knowledge could be obtained that is not possible from a single gait such as biped PDW.

Therefore, the objective of this research paper is to understand the common principle underlying PDW and PDR to clarify the elementary principles of passive dynamic locomotion. In particular, we focus on *phase transition phenomenon* between PDW and PDR [11] as well as the period-doubling bifurcation phenomenon observed in PDW. The reason why we have taken these phenomena is that these allow us to extract the common mechanism of adaptive function underlying gait transition from PDW to PDR and one-period PDW to two-period PDW. More specifically, in this research analytical Poincaré maps are derived based on the techniques of [5], [6] relating to these phenomena, and these were used in an attempt to derive and understand the stabilization mechanisms behind these phenomena. The results of this analysis show that a feedback structure equivalent to *two-delay feedback control* [12] is an inherent stabilization mechanism in PDR appearing from a model with elastic elements (Model 1), and two-period and four-period PDW appearing from stiff legs (Model 2). Furthermore, these results indicate that a common principle where the stabilization mechanism changes from a single input feedback structure to two-delay feedback structure underlies the phase transition and period-doubling bifurcation phenomena observed in models having different physical characteristics. This mechanism is the key to adaptive function underlying phase transition phenomenon between PDW and PDR and period-doubling bifurcation phenomenon in PDW. In addition, we must pay attention to the fact that, among natural phenomena such as PDW and PDR that appear according to the laws of physics, the stabilization structure explained by two-delay feedback control developed as an artificial control structure in the field of control theory is implicit.

## II. PHASE TRANSITION BETWEEN PDW AND PDR

### A. Model 1: PDW and PDR Model with Elastic Elements

In this paper, the common principle underlying passive dynamic locomotion is discussed using models (Model 1 and Model 2) that have different physical characteristics. In this section, we will attempt to elucidate stabilization mechanism and adaptive function underlying phase transition

D. Owaki and A. Ishiguro are with Department of Electrical and Communication Engineering, Tohoku University, Sendai, Japan {owaki@cmplx./ishiguro@}ecei.tohoku.ac.jp

K. Osuka is with Department of Mechanical Engineering, Osaka University, Osaka, Japan osuka@mech.eng.osaka-u.ac.jp

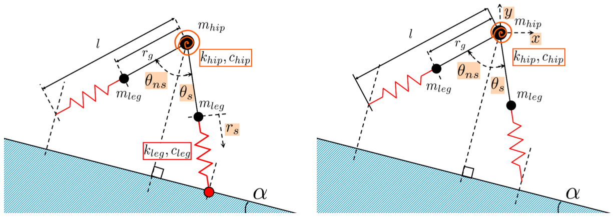

(a) Stance phase (b) Flight phase

Fig. 1. PDW and PDR model with elastic elements

from PDW to PDR, which are derived from a model with elastic elements.

Fig. 1 shows the PDW and PDR model with elastic elements (Model 1) used in this report. Running motion is described as the motion that switches between periods of *single-stance* and *flight* phases, while walking motion is described as the motion of repetition of *single-stance* phase. For simplicity, we don't consider *double-stance* phase observed in human walking in this report, assuming that the double-stance phase duration is sufficiently short. Therefore, PDW and PDR can be modeled by conceptualizing a model with the two phases shown in (a) single-stance phase (hereafter stance phase) and (b) flight phase of this figure. Motion is expressed as the motion of three centers of mass for the hip and the two legs. The body parameters are also shown in this figure. $\alpha$ denotes the angle of ground slope. A salient feature of this model is that the stance-legs are equipped with linear springs and dampers, while the hip joint is equipped with torsion spring and damper.

*1) Equations of Motion of Each Phase:* The nonlinear equations of motion of the stance and flight phases can be expressed using the Euler–Lagrange method (refer to [10]). Here, we defined that $\boldsymbol{\theta}_{es} = [\theta_{ns}, \theta_s, r_s]^T$, $\boldsymbol{\theta}_{ef} = [\theta_{ns}, \theta_s, x, y]^T$ are the state vectors for stance and flight phases, respectively. $\theta_{ns}$, $\theta_s$ represent the angles of the swing-leg and stance-leg with respect to the ground slope in the stance phase, and the angle of each swing-leg in the flight phase (differentiated by the state of the previous stance phase). $r_s$ in the stance phase represents the displacement of the linear spring in the direction of leg, and $r_s$ is zero when a leg touches the ground slope. Furthermore, in stance phase, the foot of the stance-leg is assumed to be fixed on the ground slope and is treated as a hinge joint. At the same time, in flight phase, $x$ and $y$ represent the position of the mass center of the hip. Taking $\boldsymbol{x}_{es} = [\boldsymbol{\theta}_{es}\ \ \dot{\boldsymbol{\theta}}_{es}]^T$ and $\boldsymbol{x}_{ef} = [\boldsymbol{\theta}_{ef}\ \ \dot{\boldsymbol{\theta}}_{ef}]^T$, nonlinear equations of motion are linearized around $\boldsymbol{x}_{es} = \boldsymbol{0}, \boldsymbol{x}_{ef} = \boldsymbol{0}$, we get the following linearized equations of motion:

$$\dot{\boldsymbol{x}}_{es} = \boldsymbol{A}_{es}\boldsymbol{x}_{es} + \boldsymbol{b}_{es}, \tag{1}$$

$$\dot{\boldsymbol{x}}_{ef} = \boldsymbol{A}_{ef}\boldsymbol{x}_{ef} + \boldsymbol{b}_{ef}. \tag{2}$$

*2) Geometric Constraint Conditions and State Variable Transition Rules:* Since PDW and PDR are modeled by discrete repetition of stance phases and discrete switching between stance and flight phases, it is essential to derive geometric constraint conditions in phase switching and state variables transition rules that correlate phase variables consistently. Although details of the derivation method have been

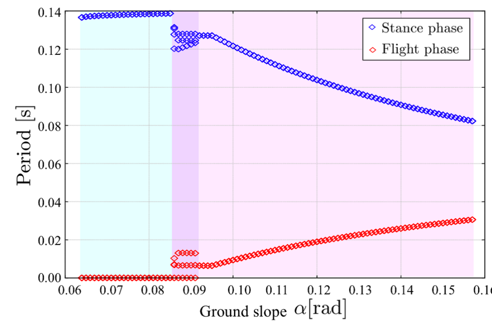


Fig. 2. Phase transition between PDW and PDR.

omitted in this report, a short description is given below (refer to [10]).

*Jumping* from the ground slope occurs while transitioning from stance phase to flight phase while running:

$$C_{erf}(\boldsymbol{x}_{es}^-) = 0, \tag{3}$$

$$\boldsymbol{x}_{ef}^+ = \boldsymbol{R}_{erf}(\boldsymbol{x}_{es}^-). \tag{4}$$

(3) shows geometric constraint condition and (4) shows state variable transition rule. Here, $\boldsymbol{x}_{es}^-$ represents the state of stance phase just before the jumping, and $\boldsymbol{x}_{ef}^+$ represents the state of flight phase just after the jumping.

State transition occurs at *landing* on the groud slope satisfies the following geometric constraint conditions during shift from flight phase to stance phase in running, and shift from stance phase to stance phase in walking:

$$C_{ers}(\boldsymbol{x}_{ef}^-) = 0, \tag{5}$$

$$C_{ews}(\boldsymbol{x}_{es}^-) = 0. \tag{6}$$

Furthermore, the corresponding state variable transition rules are expressed by the following equations:

$$\boldsymbol{x}_{es}^+ = \boldsymbol{R}_{ers}(\boldsymbol{x}_{ef}^-), \tag{7}$$

$$\boldsymbol{x}_{es}^+ = \boldsymbol{R}_{ews}(\boldsymbol{x}_{es}^-). \tag{8}$$

Here, $\boldsymbol{x}_{es}^+$ represents the state of stance phase just after the landing, $\boldsymbol{x}_{ef}^-$ is the state of flight phase just before the landing, and $\boldsymbol{x}_{es}^-$ is the state of stance phase just before the landing.

## B. Simulation Results

In numerical experiments, nonlinear equations of motion were numerically integrated using a fourth order Runge-Kutta with integration step $\Delta t = 1.0 \times 10^{-5}$ s. Fig. 2 shows the time of stance and flight phases in a steady gait shown by the robot of Model 1 at various ground slope angles (refer to video attachment). It depends on initial condition whether a gait converges to steady state or not. This figure shows that it exhibited PDW (time of flight phase is 0) at $\alpha = 0.064 \sim 0.085$ rad as a steady gait, then moved to a gait where both PDW and PDR are mixed (walking, walking, running are repeated for every three periods) at $\alpha = 0.086 \sim 0.091$ rad, and then exhibited PDR (flight phase is present) at $\alpha = 0.092 \sim 0.0157$ rad. Therefore, it can be said that this model exhibits PDW, a gait at which there is a mixture of PDW and PDR, and a gait such as PDR in an emergent manner according to ground slope angle. Moreover, this can also be understood as a type of phase transition phenomenon where transition from PDW to PDR occurs with respect to changes in slope angle. This phenomenon is discussed below by performing theoretical analysis using Poincaré map. The body parameters of this model are as follows: $K_{leg} = k_{leg}/(m_{hip}l^2) = 750$ 1/s$^2$, $K_{hip} = k_{hip}/(m_{hip}l^2) = 25.0$ 1/s$^2$, $l = 0.30$ m, $m_{hip} = 10.0$ kg, $C_{leg} = c_{leg}/(m_{hip}l^2) = 9.00$ 1/ms, $C_{hip} = c_{hip}/(m_{hip}l^2) = 0.00, \xi = m_{leg}/m_{hip} = 0.200$, $\eta = r_g/l = 0.50$.

### C. Theoretical Analysis using Poincaré Map

As a method of stability analysis, we adopted a method that uses an analytical Poincaré map [5], [6], [7], [13]. To be more precise, we performed analysis using the following procedure: (1) Derive linearized Poincaré map; (2) Eigenvalue analysis (comparison with simulation results); and (3) Derive and interpret the stabilization mechanism underlying Poincaré map.

*1) Derivation of Poincaré Map Related to Impact Points:* In this paper, the state just before the leg touches the ground slope is called the *impact point*, i.e., in PDW, the impact point is the state of stance phase and in PDR it is the state of flight phase. Taking the impact point and period in the steady gait to be $\boldsymbol{x}_*^-, \tau_*$, respectively, the state deviation at the $(k)$th impact point becomes $\Delta\boldsymbol{x}_{(k)}^- := \boldsymbol{x}_{(k)}^- - \boldsymbol{x}_*^-$. Therefore, we can define a function (Poincaré map) that transfers $\Delta\boldsymbol{x}_{(k-1)}^-$ to $\Delta\boldsymbol{x}_{(k)}^-$:

$$\Delta\boldsymbol{x}_{(k)}^- = \boldsymbol{P}_{(k)}(\Delta\boldsymbol{x}_{(k-1)}^-). \tag{9}$$

Since the applicable system is a linear system that includes state jump, the mapping $\boldsymbol{P}_{(k)}$ becomes nonlinear. We therefore take the Taylor expansion of the above formula around $\boldsymbol{x}_{(k)}^- = \boldsymbol{x}_*^-$:

$$\Delta\boldsymbol{x}_{(k)}^- = \left.\frac{\partial \boldsymbol{P}_{(k)}}{\partial \boldsymbol{x}}\right|_{\Delta\boldsymbol{x}_{(k)}^-=0} \Delta\boldsymbol{x}_{(k-1)}^- + o(\|\Delta\boldsymbol{x}_{(k)}^-\|).$$

By analyzing this linear component $\tilde{\boldsymbol{P}}_{(k)} := \left.\frac{\partial \boldsymbol{P}_{(k)}}{\partial \boldsymbol{x}}\right|_{\Delta\boldsymbol{x}_{(k)}^-=0}$, the local stability of PDW and PDR can be analyzed. We derived the following theorems from the linearized equations of motion (1), (2), the geometric constraint conditions between each phase (3) (5) (6), and the state variable transition rules between each phase (4) (7) (8):

*Theorem 1:* Linearized Poincaré map $\tilde{\boldsymbol{P}}_{walk(k)}$ of PDW (Model 1) can be expressed by the following equation:

$$\tilde{\boldsymbol{P}}_{walk(k)} = \left(\boldsymbol{I} - \frac{\boldsymbol{v}_{es*}^- \boldsymbol{C}_{ewsd}}{\boldsymbol{C}_{ewsd}\boldsymbol{v}_{es*}^-}\right) e^{\boldsymbol{A}_{es}\tau_{es*}} \boldsymbol{R}_{ewsd}, \tag{10}$$

where $\boldsymbol{R}_{ewsd}, \boldsymbol{C}_{ewsd}$ are linear components of $\boldsymbol{R}_{ews}(\boldsymbol{x}_{es}), C_{ews}(\boldsymbol{x}_{es})$ around $\boldsymbol{x}_{es} = \boldsymbol{x}_{es*}^-$ ($\left.\frac{\partial \boldsymbol{R}_{ews}(\boldsymbol{x}_{es})}{\partial \boldsymbol{x}_{es}}\right|_{\boldsymbol{x}_{es}=\boldsymbol{x}_{es*}^-}$, $\left.\frac{\partial C_{ews}(\boldsymbol{x}_{es})}{\partial \boldsymbol{x}_{es}}\right|_{\boldsymbol{x}_{es}=\boldsymbol{x}_{es*}^-}$). Here, the impact point of PDW was taken to be the state $\boldsymbol{x}_{es*}^-$ of stance phase just before landing, and the walking period of PDW was taken to be $\tau_* = \tau_{es*}$ (the period of the stance phase) in steady gait. Furthermore, $\Delta\boldsymbol{x}_{(k)}^- = \Delta\boldsymbol{x}_{s(k)}^- := \boldsymbol{x}_{es(k)}^- - \boldsymbol{x}_{es*}^-, \boldsymbol{v}_{es*} = \boldsymbol{A}_{es}\boldsymbol{x}_{es*} + \boldsymbol{b}_{es}$.

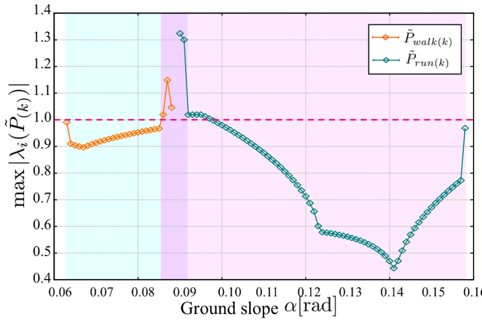


Fig. 3. Eigenvalue analysis of phase transition.

*(Proof):* Since the linearized Poincaré map of PDW can be explained in a similar manner to [6], the proof has been omitted in this paper.

*Theorem 2:* Linearized Poincaré map $\tilde{\boldsymbol{P}}_{run(k)}$ of PDR (Model 1) can be expressed by the following equation:

$$\tilde{\boldsymbol{P}}_{run(k)} = \left(\boldsymbol{I} - \frac{\boldsymbol{v}_{ef*}^- \boldsymbol{C}_{ersd}}{\boldsymbol{C}_{ersd}\boldsymbol{v}_{ef*}^-}\right) e^{\boldsymbol{A}_{ef}\tau_{ef*}} \boldsymbol{R}_{erfd} \cdot \left(\boldsymbol{I} - \frac{\boldsymbol{v}_{es*}^- \boldsymbol{C}_{erfd}}{\boldsymbol{C}_{erfd}\boldsymbol{v}_{es*}^-}\right) e^{\boldsymbol{A}_{es}\tau_{es*}} \boldsymbol{R}_{ersd}, \tag{11}$$

where $\boldsymbol{R}_{ersd}$, $\boldsymbol{C}_{ersd}$ are linear components of $\boldsymbol{R}_{ers}(\boldsymbol{x}_{ef})$, $C_{ers}(\boldsymbol{x}_{ef})$ around $\boldsymbol{x}_{ef} = \boldsymbol{x}_{ef*}^-$, and $\boldsymbol{R}_{erfd}$, $\boldsymbol{C}_{erfd}$ are linear components of $\boldsymbol{R}_{erf}(\boldsymbol{x}_{es})$, $C_{erf}(\boldsymbol{x}_{es})$ around $\boldsymbol{x}_{es} = \boldsymbol{x}_{es*}^-$. Here, the impact point of PDR was assumed to be the state $\boldsymbol{x}_{ef*}^-$ of the flight phase just before landing, the *jumping point* of PDR, which is the state just before the leg jumps off the ground slope, was assumed to be the state $\boldsymbol{x}_{es*}^-$ of the stance phase just before jumping, and the running period of PDR was assumed to be $\tau_* = \tau_{es*} + \tau_{ef*}$ (the sum of the period $\tau_{es*}$ of the stance phase and the period $\tau_{ef*}$ of the flight phase) in steady gait. Furthermore, $\Delta\boldsymbol{x}_{(k)}^- = \Delta\boldsymbol{x}_{ef(k)}^- := \boldsymbol{x}_{ef(k)}^- - \boldsymbol{x}_{ef*}^-, \boldsymbol{v}_{es*} = \boldsymbol{A}_{es}\boldsymbol{x}_{es*} + \boldsymbol{b}_{es}, \boldsymbol{v}_{ef*} = \boldsymbol{A}_{ef}\boldsymbol{x}_{ef*} + \boldsymbol{b}_{ef}$.

*(Proof):* Although the proof has not been included in this paper, a map of the stance and flight phases (stance phase: $\Delta\boldsymbol{x}_{ef(k-1)}^- \to \Delta\boldsymbol{x}_{es(k)}^-$, flight phase: $\Delta\boldsymbol{x}_{es(k)}^- \to \Delta\boldsymbol{x}_{ef(k)}^-$) can be obtained by developing a formula similar to that for PDW, and the Poincaré map can be shown using their multiplication.

*2) Eigenvalue Analysis:* Using the linearized Poincaré map given in *Theorem 1* and *Theorem 2*, the stability of PDW and PDR obtained from Fig. 2 is examined. In Fig. 3, $\max|\lambda_i(\tilde{\boldsymbol{P}}_{walk(k)})|$ at $\alpha = 0.064 \sim 0.088$ rad and $\max|\lambda_i(\tilde{\boldsymbol{P}}_{run(k)})|$ at $\alpha = 0.090 \sim 0.0157$ rad have been plotted. There seems to be small differences between simulation and theoretical results depending on linearization in dynamics and Pincaré maps. For the slope angle at which the gait transits from PDW to PDR (around 0.090 rad), the Poincaré map of PDW is unstable whereas that of PDR is stable. As a result of this, although the gait is unstable for PDW it becomes stable for PDR, leading to transition from PDW to PDR. From this figure we can verify that phase transition from PDW to PDR is exhibited due to the actualization of the most stable Poincaré map in response to the groud slope angle. Furthermore, in the gait where both PDW and PDR are mixed, the Poincaré map of neither PDW

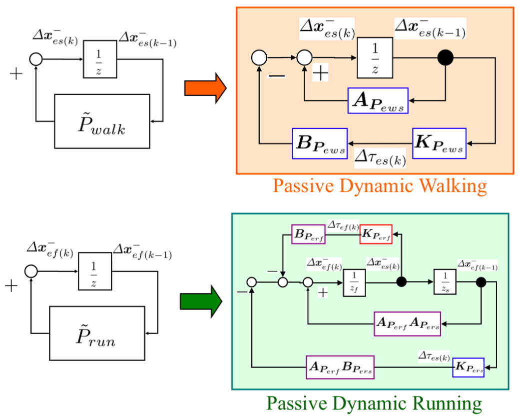


Fig. 4. Implicit feedback structure in PDW and PDR.

nor PDR has stabilized. In this gait, if Poincaré map of three periods is taken to be $\tilde{\boldsymbol{P}} = \boldsymbol{P}_{run(k+2)} \cdot \boldsymbol{P}_{run(k+1)} \cdot \boldsymbol{P}_{walk(k)}$, then it can be considered to be a stable function.

*3) Feedback Structures in the Poincaré Maps:* Based on the result of previous section's eigenvalue analysis about selecting the most stable Poincaré map, we will discuss the stabilization mechanism underlying the Poincaré maps. For the Poincaré map in PDW, substituting

$$\boldsymbol{A}_{\boldsymbol{P}_{ews}} = e^{\boldsymbol{A}_{\boldsymbol{es}}\tau_{es*}}\boldsymbol{R}_{ewsd}, \boldsymbol{B}_{\boldsymbol{P}_{ews}} = \boldsymbol{v}_{es*}^{-},$$
$$\boldsymbol{K}_{\boldsymbol{P}_{ews}} = (\boldsymbol{C}_{ewsd}\boldsymbol{v}_{es*}^{-})^{-1}\boldsymbol{C}_{ewsd}\ e^{\boldsymbol{A}_{\boldsymbol{es}}\tau_{es*}}\boldsymbol{R}_{ewsd},$$

from [6] in *Theorem 1*, we obtain

$$\Delta\boldsymbol{x}_{es(k)}^{-} = \boldsymbol{A}_{\boldsymbol{P}_{ews}}\Delta\boldsymbol{x}_{es(k-1)}^{-} + \boldsymbol{B}_{\boldsymbol{P}_{ews}}\Delta\tau_{es(k)}, \quad (12)$$
$$\Delta\tau_{es(k)} = -\boldsymbol{K}_{\boldsymbol{P}_{ews}}\Delta\boldsymbol{x}_{es(k-1)}^{-}. \quad (13)$$

In other words, it can be said that $\boldsymbol{P}_{walk(k)}$ corresponds to a discrete system (12) in which a single feedback input (13) exists (upper diagram in Fig. 4).

At the same time, for the Poincaré map in PDR, substituting

$$\boldsymbol{A}_{\boldsymbol{P}_{ers}} = e^{\boldsymbol{A}_{\boldsymbol{es}}\tau_{es*}}\boldsymbol{R}_{ersd}, \boldsymbol{B}_{\boldsymbol{P}_{ers}} = \boldsymbol{v}_{es*}^{-},$$
$$\boldsymbol{K}_{\boldsymbol{P}_{ers}} = (\boldsymbol{C}_{erfd}\boldsymbol{v}_{es*}^{-})^{-1}\boldsymbol{C}_{erfd}e^{\boldsymbol{A}_{\boldsymbol{es}}\tau_{es*}}\boldsymbol{R}_{ersd},$$
$$\boldsymbol{A}_{\boldsymbol{P}_{erf}} = e^{\boldsymbol{A}_{\boldsymbol{ef}}\tau_{ef*}}\boldsymbol{R}_{erfd}, \boldsymbol{B}_{\boldsymbol{P}_{erf}} = \boldsymbol{v}_{ef*}^{-},$$
$$\boldsymbol{K}_{\boldsymbol{P}_{erf}} = (\boldsymbol{C}_{ersd}\boldsymbol{v}_{ef*}^{-})^{-1}\boldsymbol{C}_{ersd}e^{\boldsymbol{A}_{\boldsymbol{ef}}\tau_{ef*}}\boldsymbol{R}_{erfd},$$

from *Theorem 2*, we obtain

$$\Delta\boldsymbol{x}_{es(k)}^{-} = \boldsymbol{A}_{\boldsymbol{P}_{ers}}\Delta\boldsymbol{x}_{ef(k-1)}^{-} + \boldsymbol{B}_{\boldsymbol{P}_{ers}}\Delta\tau_{es(k)}, \quad (14)$$
$$\Delta\tau_{es(k)} = -\boldsymbol{K}_{\boldsymbol{P}_{ers}}\Delta\boldsymbol{x}_{ef(k-1)}^{-}, \quad (15)$$
$$\Delta\boldsymbol{x}_{ef(k)}^{-} = \boldsymbol{A}_{\boldsymbol{P}_{erf}}\Delta\boldsymbol{x}_{es(k)}^{-} + \boldsymbol{B}_{\boldsymbol{P}_{erf}}\Delta\tau_{ef(k)}, \quad (16)$$
$$\Delta\tau_{ef(k)} = -\boldsymbol{K}_{\boldsymbol{P}_{erf}}\Delta\boldsymbol{x}_{es(k)}^{-}. \quad (17)$$

Here, substituting (16) into (14) gives

$$\Delta\boldsymbol{x}_{ef(k)}^{-} = \boldsymbol{A}_{\boldsymbol{P}_{erf}}\boldsymbol{A}_{\boldsymbol{P}_{ers}}\Delta\boldsymbol{x}_{ef(k-1)}^{-} + \boldsymbol{A}_{\boldsymbol{P}_{erf}}\boldsymbol{B}_{\boldsymbol{P}_{ers}}\Delta\tau_{es(k)} + \boldsymbol{B}_{\boldsymbol{P}_{erf}}\Delta\tau_{ef(k)}, \quad (18)$$
$$\Delta\tau_{es(k)} = -\boldsymbol{K}_{\boldsymbol{P}_{ers}}\Delta\boldsymbol{x}_{ef(k-1)}^{-}, \quad (19)$$
$$\Delta\tau_{ef(k)} = -\boldsymbol{K}_{\boldsymbol{P}_{erf}}\Delta\boldsymbol{x}_{es(k)}^{-}. \quad (20)$$

That is, it can be said that $\boldsymbol{P}_{run(k)}$ corresponds to a discrete system (18) in which the feedback structure comprised of the two inputs (19) and (20) is implicit (lower diagram in Fig. 4). $z_s^{-1}, z_f^{-1}$ in the figure are taken to be operators that delay $\tau_{es*}, \tau_{ef*}$, respectively, $z^{-1} = z_s^{-1}z_f^{-1}$ ). The feedback structure underlying PDR can be interpreted as a structure equivalent to *two-delay feedback control* [12] proposed by Mita et al. for digital control, which not only inputs the state of a sample point ($\Delta\tau_{es(k)}$), but also the state between sample points ($\Delta\tau_{ef(k)}$) as feedback inputs. In addition, regarding the ground slope angles at which walking motion cannot continue because of destabilization of stabilizing structure of PDW (greater than 0.090 [rad]), it can be presumed that the stabilizing mechanism by two-delay feedback control structure is actualized as PDR and phase transition phenomenon from PDW to PDR is observed. Therefore, in the PDW and PDR model with elastic elements (Model 1), the mechanism of transition of stable feedback structure from a single input feedback to two-delay feedback is intrinsic as an adaptive function.

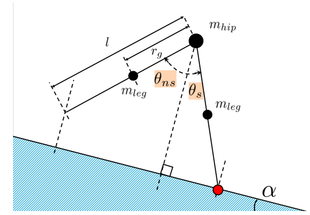

Fig. 5. PDW model with stiff legs

## III. PERIOD-DOUBLING BIFURCATION IN PDW

In this section, based on our knowledge that the stabilization mechanism equivalent to the two-delay feedback structure is present behind PDR, we attempt a new way of interpreting the period-doubling bifurcation phenomenon in PDW, which has already been discussed so far [7].

### A. Model 2: PDW Model with Stiff Legs

Fig. 5 shows a model of PDW in which the legs are modeled as a rigid body (Model 2, hereinafter called PDW model with stiff legs). This model is comparable to models that have been generally used in research works in past [1], [5], [6]. The body parameters are also shown in Fig. 5

*1) Equations of Motion:* Linear equation of motion for the stance phase, the geometric constraint conditions at the impact point, and the state variable transition rule can be described using the following equations (refer to [5], [6]):

$$\dot{\boldsymbol{x}}_{ss} = \boldsymbol{A}_{ss}\boldsymbol{x}_{ss} + \boldsymbol{b}_{ss}, \quad (21)$$
$$C_{sws}(\boldsymbol{x}_{ss}^{-}) = 0, \quad (22)$$
$$\boldsymbol{x}_{ss}^{+} = \boldsymbol{R}_{sws}(\boldsymbol{x}_{ss}^{-}). \quad (23)$$

Here, $\boldsymbol{\theta}_{ss} = [\theta_{ns}, \theta_s]^T$ represents the state vector with respect to stance phase, which is set to $\boldsymbol{x}_{ss} = [\boldsymbol{\theta}_{ss}\ \dot{\boldsymbol{\theta}}_{ss}]^T$. Equation (21) is a linear equation of motion around $\boldsymbol{x}_{ss} = \boldsymbol{0}$. Furthermore, $\boldsymbol{x}_{ss}^{+}$ represents the state of the stance phase just after landing, and $\boldsymbol{x}_{ss}^{-}$ represents the state of the stance phase just before landing.

### B. Simulation Results

In numerical experiments, nonlinear equations of motion were numerically integrated using a fourth order Runge-Kutta with integration step $\Delta t = 1.0 \times 10^{-5}$ s. Fig. 6 shows the walking period (time of stance phase) in a steady gait

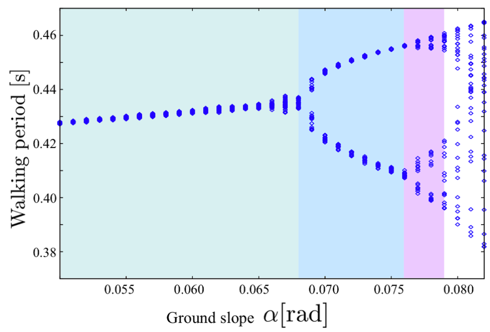

Fig. 6. Period-doubling bifurcation phenomenon in PDW.

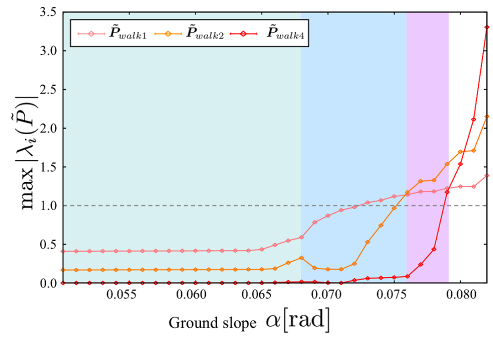

Fig. 7. Eigenvalue analysis of period-doubling bifurcation phenomenon.

demonstrated by the robot of Model 2 at various ground slope angles. From this figure, we can verify that this model exhibits one-period PDW at $\alpha = 0.050 \sim 0.068$ rad, two-period PDW at $\alpha = 0.069 \sim 0.076$ rad, and four-period PDW at $\alpha = 0.077 \sim 0.079$ rad, depending on the slope angle. In addition, it also exhibits a chaotic gait (near $\alpha = 0.082$ rad). This can also be considered as a type of period-doubling bifurcation phenomenon where it diverges from one-period PDW to two-period and four-period PDW in response to changes in slope angle. The body parameters of this model were kept the same except for the springs and dampers: $l = 0.30$ m, $m_{hip} = 10.0$ kg, $\xi = m_{leg}/m_{hip} = 0.200$, $\eta = r_g/l = 0.50$.

### C. Theoretical Analysis using Poincaré Map

In this section, we analyze the simulation results of section III-B using the same method as used in section II-C.

*1) Derivation of Poincaré Map Related to Impact Point :* From the linearized equation of motion (21), the geometric constraint condition between phases (22), and the state variable transition rule (23), we derived the following theorem regarding one-period PDW, two-period PDW, and four-period PDW occurring in Model 2:

*Theorem 3:* Linearized Poincaré maps $\tilde{\boldsymbol{P}}_{walk1(k)}, \tilde{\boldsymbol{P}}_{walk2(k)}, \tilde{\boldsymbol{P}}_{walk4(k)}$ of one-period PDW, two-period PDW, and four-period PDW (Model 2) can be expressed using the following equations:

$$\tilde{\boldsymbol{P}}_{walk1(k)} = \boldsymbol{P}_{w1} \quad (24)$$

$$\tilde{\boldsymbol{P}}_{walk2(k)} = \boldsymbol{P}_{w2}\boldsymbol{P}_{w1} \quad (25)$$

$$\tilde{\boldsymbol{P}}_{walk4(k)} = \boldsymbol{P}_{w4}\boldsymbol{P}_{w3}\boldsymbol{P}_{w2}\boldsymbol{P}_{w1} \quad (26)$$

$$\boldsymbol{P}_{w(i)} = \left(\boldsymbol{I} - \frac{\boldsymbol{v}^-_{ss(i)*}\boldsymbol{C}_{swsd(i)}}{\boldsymbol{C}_{swsd(i)}\boldsymbol{v}^-_{ss(i)*}}\right)e^{\boldsymbol{A}_{ss}\tau_{ss(i)*}}\boldsymbol{R}_{swsd(i)},$$

$$i = 1, 2, 3, 4,$$

where $\boldsymbol{R}_{swsd(i)}$ and $\boldsymbol{C}_{swsd(i)}$ are linear components of $\boldsymbol{R}_{sws}(\boldsymbol{x}_{ss})$,$\boldsymbol{C}_{sws}(\boldsymbol{x}_{ss})$ around $\boldsymbol{x}_{ss} = \boldsymbol{x}^-_{ss(i)*}$. We also assume that $\boldsymbol{v}_{ss(i)*} = \boldsymbol{A}_{ss}\boldsymbol{x}_{ss(i)*} + \boldsymbol{b}_{ss}$. Here, the impact point of PDW is taken to be the state $\boldsymbol{x}^-_{ss}$ of the stance phase just before landing (in sequence of $\boldsymbol{x}^-_{ss1*}, \boldsymbol{x}^-_{ss2*}, \boldsymbol{x}^-_{ss3*}, \boldsymbol{x}^-_{ss4*}$ from ($k$)th walk), From ($k$)th walk onwards, the walking period of PDW is taken to be $\tau_{(i)*} = \tau_{ss(i)*}$ for the ($i$)th period (period of stance phase).

*(Proof):* For the method for deriving the linearized Poincaré map of one-, two-, and four-period PDW of Model 2, refer to [7].

*2) Eigenvalue Analysis:* Using the linearized Poincaré map shown in *Theorem 3*, we examined the stability of PDW obtained in Fig. 6. In Fig. 7 $\max|\lambda_i(\tilde{\boldsymbol{P}}_{walk1(k)})|, \max|\lambda_i(\tilde{\boldsymbol{P}}_{walk2(k)})|, \max|\lambda_i(\tilde{\boldsymbol{P}}_{walk4(k)})|$ are plotted against various slope angles. From this figure, for the slope angle at which the gait diverges from one-period PDW to two-period PDW (around $\alpha = 0.068$ rad), the condition that destabilizes the Poincaré map of one-period PDW can be verified. At the same time, the Poincaré map of two-period PDW is stable at this slope angle. Consequently, although the gait is unstable for one-period PDW it becomes stable for two-period PDW because of these stabilities of Poincaré maps. As a result of this, two-period PDW is exhibited. In addition, in the bifurcation region from two-period PDW to four-period PDW, although the Poincaré map is unstable for two-period PDW, it was observed that Poincaré map was stable for four-period PDW. There seems to be small differences between simulation and theoretical results depending on linearization in dynamics and Pincaré maps. In the next section, the results of this eigenvalue analysis are discussed from the perspective of the feedback structure underlying these Poincaré maps.

*3) Feedback Structure in the Poincaré Maps:* Similar to section II-C.3, the feedback structure underlying one-period PDW can be expressed as the upper diagram in Fig. 8. Regarding two-period PDW, although it has been discussed as a stable feedback structure when considered as a single discrete system during two periods in [7], we will attempt to interpret this in a new way. In this paper, the feedback structure underlying two-period PDW is reconsidered from the standpoint of two-delay feedback control observed in PDR. To be more precise, we focus on the structure underlying Poincaré map of two-period PDW obtained in *Theorem 3*:

$$\Delta\boldsymbol{x}^-_{ss(k)} = \boldsymbol{A}_{\boldsymbol{P}_{sws(k+1)}}\boldsymbol{A}_{\boldsymbol{P}_{sws(k)}}\Delta\boldsymbol{x}^-_{ss(k-1)} + \boldsymbol{A}_{\boldsymbol{P}_{sws(k+1)}}\boldsymbol{B}_{\boldsymbol{P}_{sws(k)}}\Delta\tau_{ss(k)} + \boldsymbol{B}_{\boldsymbol{P}_{sws(k+1)}}\Delta\tau_{ss(k+1)}, \quad (27)$$

$$\Delta\tau_{ss(k)} = -\boldsymbol{K}_{\boldsymbol{P}_{sws(k)}}\Delta\boldsymbol{x}^-_{ss(k-1)}, \quad (28)$$

$$\Delta\tau_{ss(k+1)} = -\boldsymbol{K}_{\boldsymbol{P}_{sws(k+1)}}\Delta\boldsymbol{x}^-_{ss(k)}. \quad (29)$$

The two-delay feedback structure in the above formula suggests that a stabilization mechanism created by a single discrete system in two periods obtained by the coupling of two destabilized one-period feedback structures is intrinsic. Similar to two-period PDW, in the case of four-period PDW also, it can be interpreted that stable walking is continued

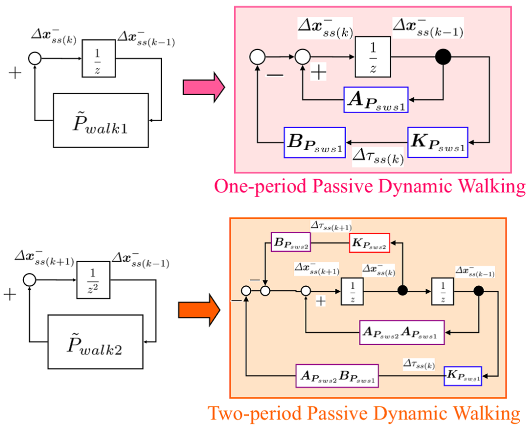


Fig. 8. Implicit feedback structure in one-period and two-period PDW.

as two destabilized two-delay structures of two-period PDW forms two-delay feedback structure as a single discrete system in four periods, i.e., in the PDW model with stiff legs (Model 2), the mechanism that keeps the walking continuing by the formation of stable feedback structure by multiplexing of two-delay structures in $2n$ periods is intrinsic as an adaptive function.

## IV. IMPLICIT TWO-DELAY FEEDBACK STRUCTURE

In this section, based on the simulation results and theoretical analyses obtained so far, we discuss the adaptive function present in common in both Model 1 and Model 2. From the simulation results, we were able to verify that the phase transition phenomenon from PDW to PDR appeared in Model 1 (Fig. 2), and the period-doubling bifurcation phenomenon appeared in Model 2 (Fig. 6) as a certain type of adaptive functions. Moreover, as a result of theoretical analyses using Poincaré maps, we verified that the phase transition phenomenon in Model 1 occurs because the feedback structure for PDW stabilization changes to a two-delay feedback structure for PDR stabilization. At the same time, regarding the period-doubling bifurcation phenomenon, gait adaptively changes because of the formation of stable feedback structure by multiplexing of two-delay feedback structure in two-period PDW, four-period PDW, and $2n$-period PDW. Based on this discussion, although the phenomena observed due to physical constraints such as differences in the physical characteristics seem to be different at first glance, it became clear that the mechanism behind these phenomena where the gait adaptively changes from PDW to PDR or one-period PDW to two-period PDW is based on the common principle of formation of stabilization mechanism due to *two-delay feedback structure* from the feedback structure of a single input.

## V. CONCLUSIONS AND FUTURE WORKS

In this paper, to understand the common principle underlying PDW and PDR, we focused on the phenomena resulting from two models having different physical characteristics and analyzed the mechanisms underlying these phenomena using analytical Poincaré map. As a result of this analysis, we verified that the adaptive function, corresponding to change in stabilization mechanism because of transition from a single input feedback structure of (one-period) PDW to two-delay feedback structure of PDR and two-period PDW comprised of double input state feedbacks, underlies the phase transition phenomenon between PDW and PDR and period-doubling bifurcation in PDW. The fact that the mechanism of two-delay feedback control, which is one of the artificially developed control structures, was found in stabilization mechanism of simple PDW and PDR models based on the laws of physics only, and also the fact that, although the phenomena exhibited due to the difference in physical characteristics seem to be different at first glance, a common stabilization strategy was found behind them are extremely interesting. In the future, we are planning to examine the design principle related to gait transition from PDW to PDR, or from one-period PDW to two-period PDW and four-period PDW and shed new light on the design principles for adaptive bipedal locomotion.

## ACKNOWLEDGMENTS

This work was supported in part by a Grant-in-Aid for Scientific Research on Priority Areas "Emergence of Adaptive Motor Function through Interaction between Body, Brain and Environment" and by Tohoku Neuroscience Global COE Basic & Translational Research Center for Global Brain Science from the Japanese Ministry of Education, Culture, Sports, Science and Technology.

## REFERENCES

[1] T. McGeer, "Passive Dynamic Walking", *The International Journal of Robotics Research*, Vol. 9, No. 2, 1990, pp.62–82.
[2] A. Goswami, B. Thuilot and B. Espau, "A Study of the Passive Gait of a Compass–like biped robot: Symmetry and Chaos", *The International Journal of Robotics Research*, Vol.17, No.12, 1998, pp.1282–1301.
[3] M. Garcia, A. Chatterjee, A. Ruina and M. Coleman, "The Simplest Walking Model: Stability, Complexity and Scaling", *ASME Journal of Biomechanical Engineering*, Vol. 120, No. 2, 1998, pp. 281–288.
[4] S. H. Collins, A. Ruina, M. Wisse, and R. Tedrake, "Efficient Bipedal Robots Based on Passive-dynamic Walkers", *Science*, Vol. 307, 2005, pp.1082–1085.
[5] K. Hirata and H. Kokane, "Stability Analysis of Linear Systems with state jump", *in Proc. of CCA2003*, 2004.
[6] Y. Sugimoto and K. Osuka, "Stability Analysis of Passive–Dynamic-Walking Focusing on The Inner Structure of Poincaré Map", *in Proc. of 12th International Conference on Advanced Robotics*, 2005.
[7] Y. Sugimoto and K. Osuka, "Hierarchical Implicit Feedback Structure in Passive Dynamic Walking", *in Proc. of the 2007 IEEE/RSJ International Conference on Intelligent Robots and Systems (IROS2007)*, 2007, pp. 2217–2222.
[8] Hirata: "On Internal Stabilizing Mechanism of Passive Dynamic Walking", *in Proc. of the 9th SICE System Integration Divirion Annual Conference*, 2008, pp.425–426.
[9] T. McGeer, "Passive Dynamic Running", *in Proc. of the Royal Society of London, Series B, Biological Science*, Vol. 240, No. 1297, 1990, pp.107–134.
[10] D. Owaki , K. Osuka, and A. Ishiguro, "On the Embodiment that Enables Passive Dynamic Bipedal Running", *in Proc. of the 2008 IEEE International Conference on Robotics and Aoutomation (ICRA2008)*, 2008, pp. 341–346.
[11] D. Owaki , K. Osuka, and A. Ishiguro, "Understanding of the Stabilization Mechanism underlying Passive Dynamic Running", *in Proc. of The 26th Annual Conference of the Robotics Society of Japan*, 2008, 3B1-09 (*in Japanese*).
[12] T. Mita, Y. Chida, Y. Kaku and H. Numasato, "Two-Delay Robust Digital Control and Its Applications –Avoiding the Problem on Unstable Limiting Zeros–", *IEEE Transactions on Automatic Control*, Vol. 35, No. 8, 1990, pp. 962–969.
[13] J. W. Grizzle, F. Plestan and G. Abba, "Poincré's Method for System with Impulse Effects: Application to Mechanical Bipedal Locomotion", *in Proc. of the 38th Conf. on Decision and Control*,1999, pp.3869–3876.